On the Effect of IF Power Nulls in Schottky Diode Harmonic Mixers

Roland Feinäugle, Heinz-Wilhelm Hübers, Hans Peter Röser, and Jeffrey L. Hesler, *Member, IEEE*

***Abstract*—Experimental results reveal the existence of a null in the IF output power for certain bias voltage levels in single Schottky diode harmonic mixers at terahertz frequencies. This dramatic loss of IF power is due to a drastic increase of conversion loss and is governed by intrinsic diode parameters, as well as external parameters. For a second harmonic mixer, this is due to a competition of two mixing paths, one is the mixing of the RF with the doubled local oscillator (LO) frequency and the other a mixing of the RF with the LO to an LO sideband followed by a second mixing with the LO, both leading to the IF. In this paper, we present a systematic investigation, as well as some basic relations between these parameters and the depth and voltage levels where the conversion loss increases. Good agreement is obtained between a simple analysis and the experimental data on second and fourth harmonic mixers.**

***Index Terms*—Harmonic mixer, Schottky diode, small-signal analysis, terahertz.**

I. Introduction

SCHOTTKY diodes have been used as mixers in a vast variety of applications for many years now, in large part due to their well-known nonlinear current/voltage (*I-V*) characteristics. Amongst others, they work as low-noise mixers in heterodyne receivers at frequencies up to 5 THz. Such highly sensitive receivers are used in areas such as radio astronomy, remote sensing of the atmosphere, and for plasma diagnostics [1].

The performance of the Schottky diode is a crucial factor in the determination of the sensitivity of a heterodyne receiver. Thus, understanding the physical and electrical behavior of the Schottky diode is crucial for implementing high-performance heterodyne receivers.

Besides a wide range of applications, Schottky diodes are also of interest for fundamental research. In order to operate at terahertz frequencies, the Schottky diode anode diameter needs to be in the submicrometer range. This implies the diode zero voltage capacitance is in the several femtofarad range. On the other hand, epitaxial doping densities of up to 10^{18} cm^{-3} are needed in order to keep the parasitic diode series resistance low and, together with the capacitance, raise the cutoff frequency to several terahertz. In general, these mesoscopic structures with depletion layer thicknesses below the electron's mean free path are suspected to have an influence on the conduction mechanism of submicrometer Schottky diodes [2], [3].

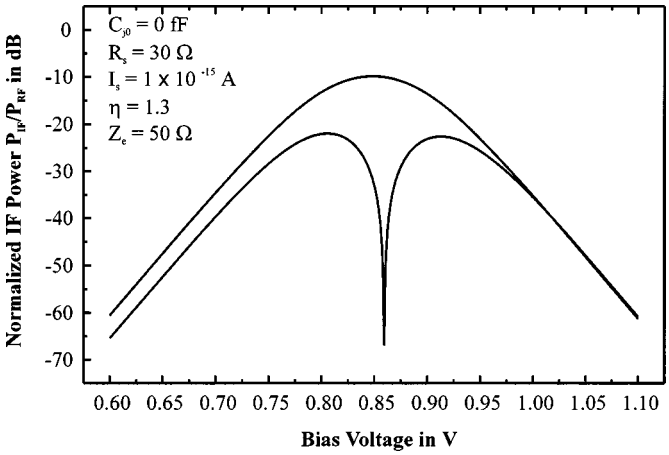

Fig. 1. Calculation of normalized IF power versus bias voltage for a typical diode. The upper curve shows a fundamental mixer pumped at an LO frequency of 693 GHz. When the same diode is operated as a second harmonic mixer, the calculated IF power shows a significant null at a certain bias voltage (lower curve). In both cases, the junction capacitance has been neglected.

Another interesting effect connected with submicrometer GaAs Schottky diodes, which, in turn, is the main focus of this paper, has been reported repeatedly by several authors [4]–[7]. Large decrease of IF power when varying the dc-bias voltage has been observed for Schottky diodes operated as mixers under certain mixing conditions. A similar phenomenon has been observed for tungsten–nickel point contact diodes [8]. Although this effect has been known for some time, only recently has a theoretical explanation been given [7], [9]. Nevertheless, a comparison of measured data with theoretical predictions needs to be carried out. Therefore, we present a detailed study of submicrometer GaAs Schottky diodes under fundamental, as well as harmonic, mixing conditions at terahertz frequencies.

Considering the case of a fundamental mixer—a mixer where the local oscillator (LO) frequency ω_{LO} is of the order of the signal frequency ω_{RF}—it is well understood that successively increasing the dc-bias voltage or the dc-bias current, respectively, results in an IF power output with one broad maximum (Fig. 1, upper curve).

In contrast, it has been observed that, under similar bias conditions, the same diode reveals a significant loss of IF power Fig. 1 (lower curve) when operated in a harmonic mixer mode at terahertz frequencies [4]–[7]. In the case of a single-diode second harmonic mixer, where the LO frequency is close to

Manuscript received July 12, 2000; revised February 14, 2001.

R. Feinäugle is with the European Astronaut Centre, D-51147 Cologne, Germany (e-mail: roland.feinaeugle@esa.int).

H.-W. Hübers is with the Institute of Space Sensor Technology and Planetary Exploration, German Aerospace Center, D-12489 Berlin, Germany.

H. P. Röser is with the Institute of Space Sensor Technology and Planetary Exploration, German Aerospace Center, D-12489 Berlin, Germany and is also with the Faculty of Mechanical Engineering and Transport Systems, Technical University of Berlin, 10623 Berlin, Germany.

J. L. Hesler is with the Department of Electrical Engineering, University of Virginia, Charlottesville, VA 22903 USA.

Publisher Item Identifier S 0018-9480(02)00026-1.

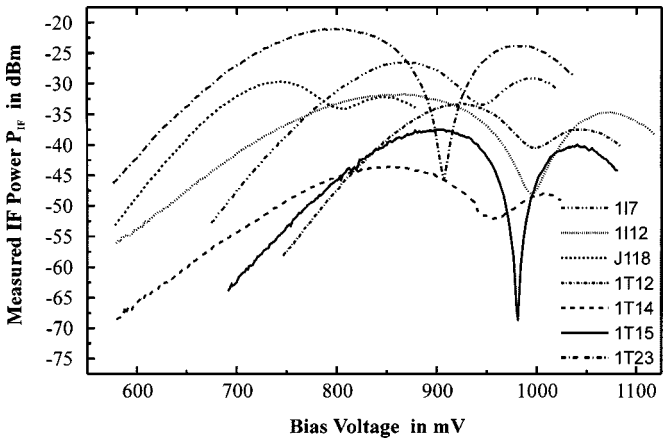

Fig. 2. Measured IF power curves versus bias voltage for real diodes whose diode parameters can be found in Table I. When driven as second harmonic mixers, all the diodes show a minimum of IF power, but at different bias voltages and with different depths.

one-half of the RF, a minimum in the IF power can be observed at different points and with different depths depending on the parameters of the investigated diode (Fig. 2).

This sharp loss of IF power can be explained by a small-signal analysis by taking into account different mixing paths for the conversion of power from the signal frequency to the IF [7], [9]. For a second harmonic mixer, the two competing mixing paths are the mixing of the RF with the doubled LO frequency and a mixing of the RF with the LO to an LO sideband (SB) followed by a second mixing with the LO, both leading to the IF.

Following a phenomenological introduction in Section II-A, this IF loss mechanism for second harmonic mixers is analyzed in Section II-B. Using this approach, it is now possible to investigate the diode and measurement parameters, which impact the depth and the bias voltage where this IF power null occurs. In Section II-C, we analyze the influence of the diode barrier capacitance. Higher (> 2) harmonic mixers are treated in Section II-D, whereas in Section II-E, the bias voltage at the IF power null is covered. In Section III-A, we explain the experimental setup. Comparison of measured and calculated curves is, therefore, possible for the first time and will be presented in Section III-B. Measurements for higher order harmonic mixers and for the voltage of the IF power null are presented in Sections III-C and III-D , respectively.

II. Theory

A. Small-Signal Analysis

It has been shown recently [7], [9] that, for a single-diode second harmonic mixer, cancellation of IF power can occur due to competition between different mixing paths. Following the notation of [10], the second harmonic mixer can be described using the admittance matrix $\mathbf{Y}$, which connects the small-signal voltages V_m and currents I_m at the different SB frequencies ω_m

$$\omega_m = |m\omega_{\mathrm{LO}} + \omega_{\mathrm{IF}}| \tag{1}$$

with ω_{LO} and ω_{IF} LO frequency and IF, respectively. For a second harmonic mixer with an exciting RF at the second upper sideband (USB) of the LO frequency ($2\omega_{\mathrm{LO}} + \omega_{\mathrm{IF}}$) and with all the lower SBs ($m < 0$), as well as SBs higher than the second ($m > 2$) shorted out, the augmented matrix $\mathbf{Y}'$ can be written as

$$\begin{bmatrix} I_2' \\ I_1' \\ I_0' \end{bmatrix} = \begin{bmatrix} Y_{22}' & Y_{21}' & Y_{20}' \\ Y_{12}' & Y_{11}' & Y_{10}' \\ Y_{02}' & Y_{01}' & Y_{00}' \end{bmatrix} \begin{bmatrix} V_2' \\ V_1' \\ V_0' \end{bmatrix}. \tag{2}$$

The augmented matrix is an admittance matrix $\mathbf{Y}$, where the embedding impedance, as well as the diode series resistance of each port, have been included in the network. Unlike a fundamental mixer, there are no *external* currents at the LO SBs ($m = 1$), hence, I_1' equals zero. Thus, the matrix (2) can be reduced to a 2×2 matrix, where V_1' has been eliminated, but the solution still depends on the admittances at these frequencies. This represents a two-port network with the two ports corresponding to the RF and IF, respectively,

$$\begin{bmatrix} I_2'' \\ I_0'' \end{bmatrix} = \begin{bmatrix} Y_{22}'' & Y_{20}'' \\ Y_{02}'' & Y_{00}'' \end{bmatrix} \begin{bmatrix} V_2'' \\ V_0'' \end{bmatrix}. \tag{3}$$

The elements of the reduced augmented matrix $\mathbf{Y}''$ are of the form

$$Y_{20}'' = Y_{20}' - \frac{Y_{21}'\, Y_{10}'}{Y_{11}'} \tag{4}$$

where Y_{20}' represents the "standard" mixing path for power converted from the RF by mixing with the second harmonic of the LO. The second term in (4) represents another mixing path from the RF to the LO USB frequency ω_1 and from there down to the IF. It can be seen from (4) that two competing mixing paths exist in a second harmonic mixer. If the paths possess the same admittance, the overall conversion efficiency will be zero. This is the result of [7] and [9].

If we insert typical diode data into (3) and apply standard harmonic-balance techniques [11] in order to derive small-signal voltages, currents, as well as mixer conversion losses, we can compute and see the decrease of conversion efficiency for certain bias conditions [9]. This method gives results with sufficient accuracy for mixer design purposes. On the other hand, by applying the numeric computations at this point, one loses insight into some important parameters governing or, at least, influencing the behavior of both fundamental and harmonic mixers. It is, therefore, helpful to carry further the analytical calculations, knowing that, at certain points, simplifications have to be made in order to keep the formalism manageable. One approximation results from the fact that, with an analytic approach, only a limited number of USBs and lower SBs can be taken into account. A further simplification is the use of approximate capacitance/voltage curves for the diode and the fact that, at terahertz frequencies, the embedding impedances cannot be determined experimentally.

B. Extended Analysis

The mixer conversion loss for the case of second harmonic down conversion L_{02} can be taken from [10]

$$L_{02} = \frac{|Z_{\mathrm{RF}} + R_{s2}|^2\ |Z_{\mathrm{IF}} + R_{s0}|^2}{4\,|Z_{02}''|\,\mathrm{Re}(Z_{\mathrm{RF}})\mathrm{Re}(Z_{\mathrm{IF}})} \tag{5}$$

with Z_{RF} and Z_{IF} the embedding impedances at the RF and IF and R_{s2} and R_{s0} the series resistances at these frequencies. Z''_{02} represents the impedance matrix element connecting the current at the exciting RF with the small-signal voltage at the IF, as shown in (6), at the bottom of this page. It can be calculated by inverting (3) and taking into account the following relationship:

$$\mathbf{ZI} = \mathbf{V}, \qquad \text{with} \quad \mathbf{Z} = \mathbf{Y}^{-1} \tag{7}$$

the impedance matrix $\mathbf{Z}$ being the inverse of the admittance matrix $\mathbf{Y}$. Z''_{02} can be evaluated using

$$Y'_{mn} = G_{m-n} + i(\omega_{\mathrm{IF}} + m\omega_{\mathrm{LO}})C_{m-n} + \delta_{mn}\frac{1}{R_{sm} + Z_{em}} \tag{8}$$

with G_m and C_m being the Fourier coefficients of the conductance G_j and the capacitance C_j of the form

$$G_m = \frac{\omega_{\mathrm{LO}}}{2\pi}\int_{-\pi/\omega_{\mathrm{LO}}}^{\pi/\omega_{\mathrm{LO}}} G_j(t)\exp\{-im\omega_{\mathrm{LO}}t\}dt \tag{9}$$

and

$$C_m = \frac{\omega_{\mathrm{LO}}}{2\pi}\int_{-\pi/\omega_{\mathrm{LO}}}^{\pi/\omega_{\mathrm{LO}}} C_j(t)\exp\{-im\omega_{\mathrm{LO}}t\}dt. \tag{10}$$

Thereby, the parameters appearing in the diode's conductance

$$G_j = \frac{d}{dV_j}I_j(V_j) = \frac{I_s e}{\eta kT}\exp\left\{\frac{eV_j}{\eta kT}\right\} \tag{11}$$

can be derived from the diode's *I-V* characteristic, which, in turn, can be measured (see Section III-A).

Assuming the diode's *C-V* characteristic is known, one can calculate the IF power of a mixer directly by applying this formalism without additional numeric means. This has been done for some typical submicrometer GaAs Schottky diodes, as shown in Fig. 1. In order not to obscure the effect of the IF power null, the zero-bias capacitance is set to zero. As mentioned earlier, one can see that the normalized IF power shows a significant dip at a certain bias voltage for a second harmonic mixer, whereas this behavior is not present for a fundamental mixer with the same diode parameters. This phenomenon is also seen in experimental investigations of harmonic mixers (Fig. 2).

In contrast to a harmonic-balance analysis, by evaluating the analytical equations it is possible to get more insight into the mixer behavior. Nevertheless, for this approach, some approximations and assumptions must be made, which may lead to slightly inaccurate results. The errors being introduced do not seem to be large, however, when the analysis is compared with measured curves.

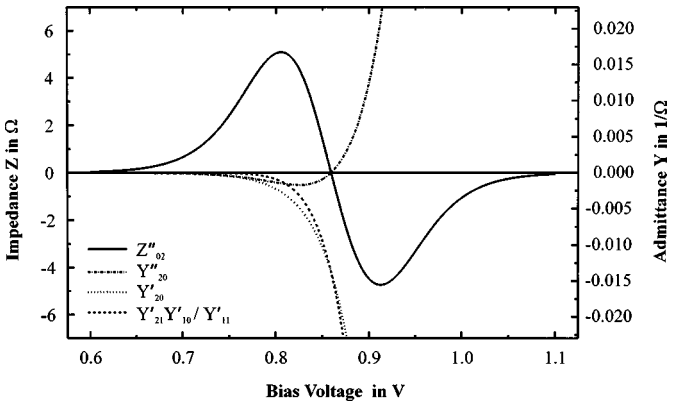

Fig. 3. Calculated diode impedance and admittance as a function of bias voltage. Two different components of the admittance matrix element of a second harmonic mixer corresponding to two different mixing paths (see text) have been plotted. At a certain bias voltage, they have the same magnitude, thus, the overall admittance matrix Y''_{20} element and the corresponding impedance matrix element Z''_{02} are zero at this voltage. The barrier capacitance has been neglected.

Looking at Fig. 3 gives evidence to the stated suggestion that the competition of different mixing paths leads to the decrease of IF power. Here, the competing admittances have been plotted separately versus bias voltage for the two different mixing paths present in a second harmonic mixer. There exists a bias voltage where both admittances have the same magnitude and, hence, cancel. This leads to an overall admittance null and, thus, to a null of the diode's impedance matrix element at exactly that bias voltage. Taking the absolute value of the impedance matrix element squared and plotting it logarithmically versus bias voltage yields a deep null in IF power (Fig. 4). The reason for not yielding negative infinite values of the IF power is due to the discrete step width of the calculated curve.

This principle of a single null in IF power for a second harmonic mixer is not an artifact of neglecting the higher harmonic SBs resulting in a truncated matrix in (2). This can be shown by numeric harmonic-balance simulations, which take into account several higher harmonics (not presented here). This can also be seen from Fig. 5 where the initial equation system (2) has been expanded by including the LO lower SB. Even though a slight modification of the calculated curve occurs, the occurrence of the conversion loss null is not affected. For a second harmonic mixer with an extended admittance matrix, still only a single IF power null is present. The same conclusion can be drawn using the rule-of-thumb given in [12], which implies that the order of magnitude for a given mixing product is G^n, where n indicates the mixing of a signal with $n\omega_{\mathrm{LO}}$ and G is the conversion gain from $n\omega_{\mathrm{LO}}+\omega_{\mathrm{IF}}$ to ω_{IF}. Applying this to (4) shows that the two mixing paths are of the same order of magnitude with $n = 2$. Expanding (2) for the inclusion of the lower LO SB still yields

$$Z''_{02} = \frac{-Y''_{02}}{Y''_{22}Y''_{00} - Y''_{02}Y''_{20}} = \frac{\left(Y'_{02} - \dfrac{Y'_{01}Y'_{12}}{Y'_{11}}\right)}{\left(Y'_{20} - \dfrac{Y'_{21}Y'_{10}}{Y'_{11}}\right)\left(Y'_{02} - \dfrac{Y'_{01}Y'_{12}}{Y'_{11}}\right) - \left(Y'_{22} - \dfrac{Y'_{21}Y'_{12}}{Y'_{11}}\right)\left(Y'_{00} - \dfrac{Y'_{01}Y'_{10}}{Y'_{11}}\right)} \tag{6}$$

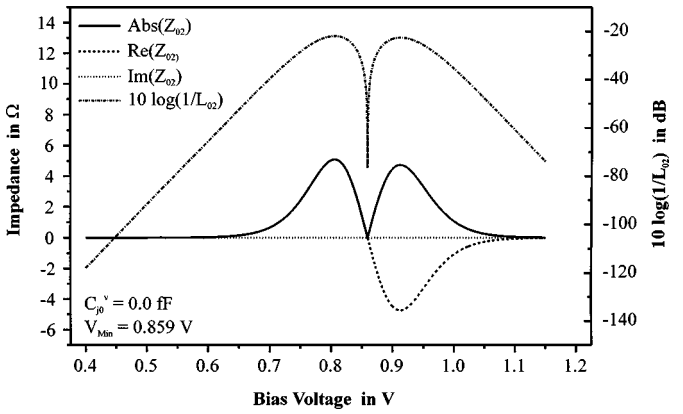

Fig. 4. Impedance and conversion loss as a function of bias voltage. When the barrier capacitance is neglected, the real part of the impedance matrix element is zero at a certain bias voltage, whereas the imaginary part is zero for all bias voltages. Calculating the (normalized) IF power according to (5), therefore, results in a deep null in IF power at this bias voltage level.

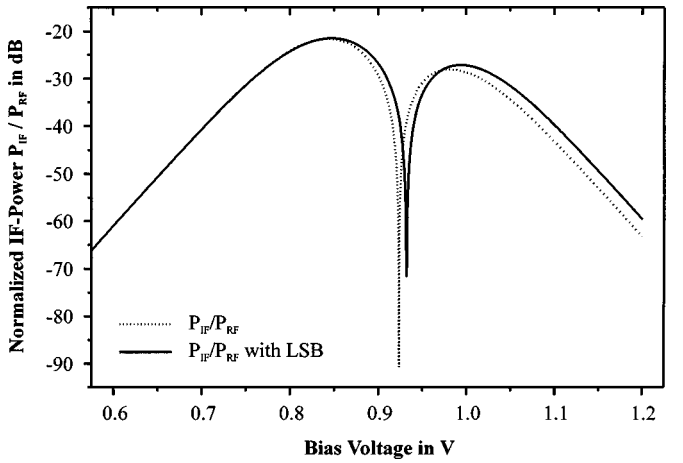

Fig. 5. Calculated IF power as a function of bias voltage for two approximations. The theoretically determined IF power changes only slightly by incorporating another SB (in this case, the LO lower SB) into the model for a second harmonic mixer.

two contributions with $n = 2$ and all the other products yielding $n > 2$.

C. Including the Diode Barrier Capacitance

Up to now, the time-varying capacitive conductance has been neglected in the analysis. Now, the effect of this capacitive variation will be considered. Typically, a dependence of the diode barrier capacitance C_j on the barrier voltage V_j of $C_j \propto (V_d - V_j)^{-1/2}$ is assumed [10]. Here, V_d represents the diode's diffusion potential. This approach yields reasonable results for small bias voltages, where the barrier is far from the flat-band condition. For forward-bias voltages near the flat-band condition, this equation gives unphysically high barrier capacitances and approaches infinite capacitances at the flat-band voltage.

To avoid this condition, one can use an approach where the common approximation of constant space charge in the depletion area with an abrupt drop of this space charge at the boundary has been given up [13]. More detailed analysis of the (majority) charge carrier distribution leads to a refined electrical field distribution in the depletion zone and its borders. This yields a modified capacitance/voltage relationship having a finite and, thus, more realistic capacitance under flat-band conditions [7]

$$C_{j,\text{refined}} = A_d \sqrt{\frac{\varepsilon_r \varepsilon_o e N_d}{2}} \times \frac{1 - \exp\left\{\dfrac{e(V_d - V_j)}{kT}\right\}}{\sqrt{V_d - V_j - \dfrac{kT}{e}\left(1 - \exp\left\{\dfrac{e(V_d - V_j)}{kT}\right\}\right)}}. \tag{12}$$

where A_d is the anode area, ε_r is the dielectric constant, ε_0 is the vacuum dielectric permittivity, and N_d is the doping density of the epitaxial layer. In order to utilize this refined, but rather complicated, capacitance equation, a numerical fit has been carried out with the following equation:

$$C_j = C_{j0}\left(1 + A\,\exp\left\{\frac{e\left(V_d - V_j - \dfrac{kT}{e}\right)}{BkT}\right\}\right). \tag{13}$$

Here, C_{j0} is the zero-bias capacitance and A and B are free parameters to fit this equation to the refined capacitance (12). With A and B having values of 3.3 and 9, respectively, (13) yields a reasonably good approximation of the refined capacitance model, as well as of the classical capacitance.

Using (13), it is now possible to take into account the effects of capacitive mixing for a harmonic mixer through (8). If the admittance matrix element and normalized IF power are calculated with the same diode parameters as in Fig. 4, but introducing a zero-voltage capacitance of 0.1 fF, the following behavior can be observed.

Looking at the real and imaginary parts of the impedance matrix elements, it can be seen that, by introducing a capacitive admittance, the impedance matrix element becomes complex. The absolute value of the impedance matrix element is no longer zero at the IF power null and, therefore, the null itself is not as deep as without capacitive elements (Fig. 4). The reason for this behavior can be found by looking at (8). By performing the Fourier transformation, it can be shown analytically that the Fourier components of the conductance G_m and the capacitance C_m are either real or imaginary for the same SB index m. Since they are connected by the complex number i, the overall admittance matrix element and, thus, the impedance matrix element, is complex whenever G_m and C_m are present at the same time. The absolute value of the complex impedance matrix element, on the other hand, is zero only if the real part, as well the imaginary part, become zero for the same bias voltage. This is no longer the case, as can be seen in Fig. 6. The addition of the capacitance still results in a minimum of the impedance matrix element, but the IF power null is not as deep. The effect explains the deep nulls in IF power at terahertz frequencies can only be measured with diodes having small zero-voltage capacitance.

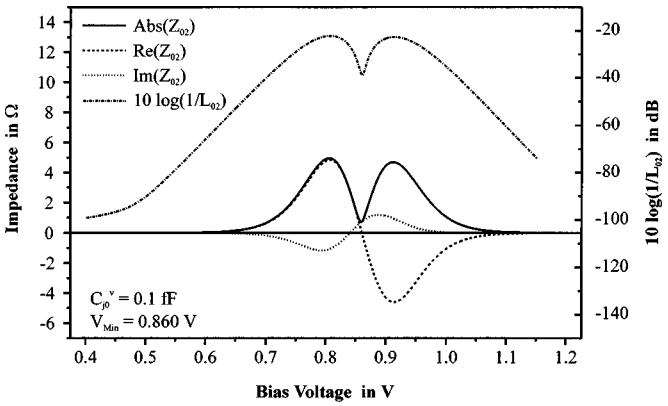

Fig. 6. Impedance and conversion loss as a function of bias voltage. Taking the same diode and measurement parameters as in Fig. 4, but introducing a zero-voltage capacitance of 0.1 fF, results in shallower IF power nulls. This is due to the fact that the impedance matrix element is not purely real anymore, but has an imaginary component. Both the real and imaginary components are not zero at the same bias voltage, thus, the absolute value of the impedance matrix element does not reach zero.

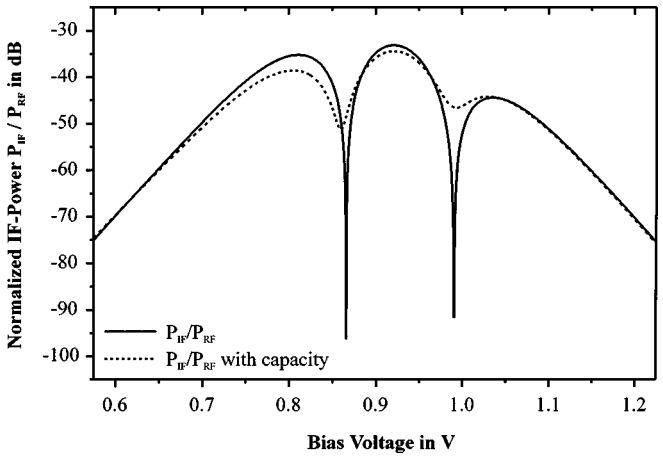

Fig. 7. Calculated normalized IF power as a function of bias voltage for a third harmonic mixer with the following diode and measurement parameters: $I_s = 8.0 \times 10^{-14}$ A, $\eta = 1.65$, $R_s = 33.6\,\Omega$, $v_{\rm LO} = 693$ GHz, $v_{\rm IF} = 11$ GHz, $C_{j0} = 0$ fF, $C_{j0} = 0.15$ fF, $Z_e = 50\,\Omega$, and $Z_e = 50 + i25\,\Omega$, respectively.

D. Higher Order Harmonic Mixers

In evaluating a third harmonic mixer—a mixer where the LO frequency is ≈ one-third of the signal frequency—one can exploit the following expression:

$$\begin{bmatrix} I_3' \\ I_2' \\ I_1' \\ I_0' \end{bmatrix} = \begin{bmatrix} Y_{33}' & Y_{32}' & Y_{31}' & Y_{30}' \\ Y_{23}' & Y_{22}' & Y_{21}' & Y_{20}' \\ Y_{13}' & Y_{12}' & Y_{11}' & Y_{10}' \\ Y_{03}' & Y_{02}' & Y_{01}' & Y_{00}' \end{bmatrix} \begin{bmatrix} V_3' \\ V_2' \\ V_1' \\ V_0' \end{bmatrix}. \tag{14}$$

Here, the augmented $\mathbf{Y}$ matrix has been expanded to 4×4 to incorporate the third USB ($3\omega_{\rm LO} + \omega_{\rm IF}$). Following the same method used for a second harmonic mixer, the *external* currents at the LO SB, as well as the second SB, can again be set to zero and (14) can be simplified by eliminating V_1' and V_2' as follows:

$$\begin{bmatrix} I_3'' \\ I_0'' \end{bmatrix} = \begin{bmatrix} Y_{33}'' & Y_{30}'' \\ Y_{03}'' & Y_{00}'' \end{bmatrix} \begin{bmatrix} V_3'' \\ V_0'' \end{bmatrix}. \tag{15}$$

This results in an admittance matrix element of the form

$$Y_{30}'' = Y_{30}' - Y_{32}' \frac{Y_{20}' - \dfrac{Y_{21}'Y_{10}'}{Y_{11}'}}{Y_{22}' - \dfrac{Y_{21}'Y_{12}'}{Y_{11}'}} + Y_{31}' \left(\frac{Y_{12}' \left(Y_{20}' - \dfrac{Y_{21}'Y_{10}'}{Y_{11}'} \right)}{Y_{11}' \left(Y_{22}' - \dfrac{Y_{21}'Y_{12}'}{Y_{11}'} \right)} - \frac{Y_{10}'}{Y_{11}'} \right) \tag{16}$$

which connects the excitation current at the third harmonic SB with the IF voltage. Rearranging (16) now yields six different mixing paths. At first sight, one would assume that the existence of a variety of mixing paths would lead to several IF power minima. Nevertheless, evaluating (15) in the same manner as for a second harmonic mixer reveals the existence of only two minima. This can be seen in Fig. 7, where the IF power for a third harmonic mixer has been calculated for some typical diode parameters with and without diode capacitance and complex embedding impedances, respectively. Looking again at the order of magnitude of the mixing products in (16) now reveals four contributions with G^3 as the strongest products and all other products contributing with $n > 3$. The existence of two minima for a third harmonic mixer and one minimum for a second harmonic mixer confirms the phenomenological law introduced in [9], i.e., that an Nth harmonic mixer produces $(N-1)$ IF power nulls. This behavior has also been confirmed through numeric harmonic balance analysis up to the order of a fifth harmonic mixer. Nevertheless, the reason behind this $N-1$ law is still not clear.

E. Voltage Position

Thus far, only the depth of the IF power null has been considered. Now, an expression will be derived to estimate the bias voltage where the IF power null occurs. Looking at (5) and (6), large conversion loss and, therefore, low IF power, occurs when Y_{02}'' is small. Thus, Y_{02}'' has been determined by calculating the corresponding matrix elements of the admittance matrix Y_{mn}' according to (8)–(11). Y_{02}'' has then been set to zero in order to solve (4) for the bias voltage. Once again, the diode capacitance has been neglected because it has only a small effect on the voltage of the IF power null. Also, including the capacitance would make it impossible to gain an analytical expression for the IF power null voltage $V_{\rm min}$. Performing the substitution in (4), the bias voltage for minimum IF power is shown in (17), at the bottom of the following page, where I_n is the modified Bessel function of the first kind and of the nth order and $V_{\rm LO}$ is the intrinsic voltage across the diode depletion layer induced by the LO. It can be seen from (17) that $V_{\rm min}$ depends on diode parameters such as the ideality factor, saturation current, series resistance, and embedding impedance, as well as externally determined parameters such as the LO power in $V_{\rm LO}$.

III. Measurements

A. Experimental Setup

The Schottky contacts investigated consist of submicrometer Pt dots on an epitaxial layer of ⟨100⟩ GaAs. The diode epitaxial layers have thicknesses between 300–1000 Å and doping densi-

TABLE I
PARAMETERS OF THE INVESTIGATED DIODES. THE VALUES FOR R_s AND η ARE MEASURED VALUES AND VARY FROM CONTACT TO CONTACT. THEY HAVE TO BE TAKEN AS TYPICAL VALUES GAINED FROM SEVERAL MEASUREMENTS. THE OTHER PARAMETERS ARE SUPPLIED BY THE MANUFACTURERS [UNIVERSITY OF VIRGINIA (UVA), MASSACHUSETTS INSTITUTE OF TECHNOLOGY (MIT)]. C_{j0} IS CALCULATED FROM THE DOPING DENSITY AND EPILAYER PARAMETERS

Diode name		**1I7**	**1I12**	**J118**	**1T12**	**1T14**	**1T15**	**1T23**
Producer		UVA	UVA	MIT	UVA	UVA	UVA	UVA
Anode diameter	d_A in μm	0.8	0.45	1.0	0.5	0.5	0.25	0.25
Doping epitaxial layer	N_d in 10^{17} cm^{-3}	3	4.5	1	3	10	10	10
Thickness epitaxial layer	w_{epi} in A	1000	600	1000	750	450	300	300
Zero-bias capacitance	C_{j0} in fF	0.9-1.2	0.45	1.8	0.5	0.85	0.25	0.5
Series resistance	R_s in Ω	13	33	30	28	10	20	30
Ideality coefficient	η	1.3	1.4	1.15	1.22	1.5	1.5	1.6

ties varying from 10^{17} cm^{-3} to 10^{18} cm^{-3}. They are grown on n^+ GaAs with a doping density of $\approx 5 \times 10^{18}$ cm^{-3}. Several thousand anodes were arranged in a honeycomb structure on a single chip with varying anode diameters down to 0.25 μm depending on the used chip. The chips were mounted in a corner-cube mixer block [1] with one of the diodes electrically contacted with an Au/Ni whisker. On the backside of the substrate, an ohmic contact was deposited. More details about the Schottky diodes and their manufacturing process can be found in [14] and [15].

The diode *I-V* curves were measured with a Keithley 236 source and measurement unit. From these curves, the diode series resistance R_s, saturation current I_s, and ideality factor η were derived by a least-squares fit of an ideal *I-V* curve, assuming a pure thermionic emission over the barrier [13]

$$I_j = I_s \exp\left\{\frac{eV_j - R_s I_j}{\eta kT}\right\}. \tag{18}$$

I_j and V_j are the diode dc current and voltage, e is the electronic charge, k is the Boltzmann constant, and T is the physical temperature. Relevant diode parameters together with some diode data provided by the manufacturer can be taken from Table I.

The diodes were measured in a setup where two CO_2 pumped far-infrared gas lasers with output powers of a few milliwatts were used as continuous-wave radiation sources (Fig. 8). The laser pumping the diode as a LO was emitting at 693 GHz, whereas the "RF" laser was operated at 1397 GHz. This resulted in an IF of 11 GHz when mixing at the second harmonic. For comparison, the diodes were also measured when operating as fundamental mixers. In this case, both lasers were coarse tuned to 2523 GHz with one laser slightly detuned to yield an IF of about 1 MHz. We also measured the diodes in fourth harmonic mixer mode. Here, the signal laser was tuned to 693 GHz, whereas the pump (LO) was provided by a klystron operating at 171.8 GHz. The resulting IF was 5.8 GHz.

The diodes were mounted in a corner-cube mixer and RF coupling was provided by the diode contact whisker. The far-infrared laser beams were focused with appropriate high-density polyethylene lenses into the corner cube in order to match the laser beams to the long-wire antenna. Since the antenna pattern of the corner cube depends on the frequency, optimal coupling can only be achieved for one frequency, nominally the signal frequency. All the measurements were performed at room temperature. The experimental setup is described in greater detail in [7].

B. Comparison of Calculated and Measured IF Power Curves

When comparing diodes with different zero-voltage capacitances (Table I), the effect of the diode barrier capacitance can

$$V_{\min} = \frac{\eta kT}{e} \ln\left\{\frac{\frac{\eta kT}{eI_s} I_2\left(\frac{eV_{\mathrm{LO}}}{\eta kT}\right)}{(R_{s1}+Z_{e1}) I_1^2\left(\frac{eV_{\mathrm{LO}}}{\eta kT}\right) - (R_{s1}+Z_{e1}) I_0\left(\frac{eV_{\mathrm{LO}}}{\eta kT}\right)\frac{\eta kT}{eI_s} I_2\left(\frac{eV_{\mathrm{LO}}}{\eta kT}\right)}\right\} \tag{17}$$

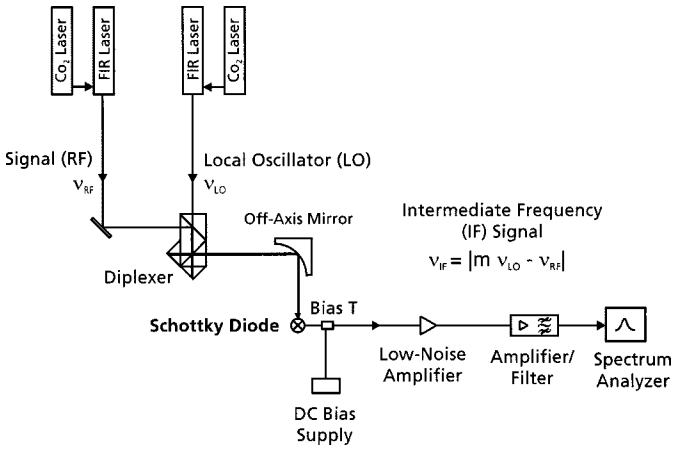

Fig. 8. Experimental setup for two laser mixing experiments.

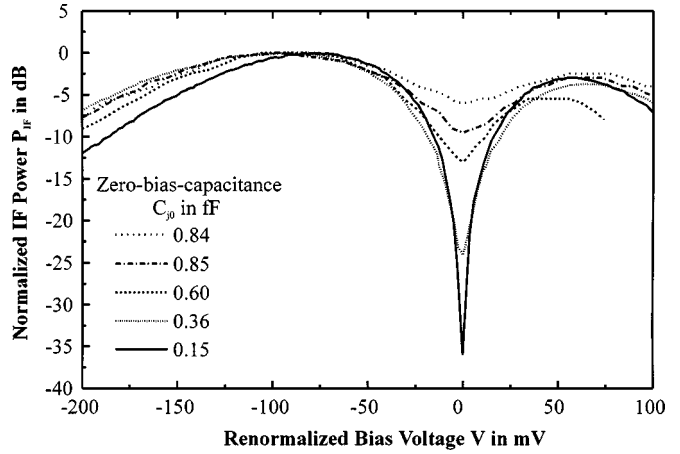

Fig. 9. Measured IF power as a function of bias voltage. Measured IF power curves have been normalized to their respective maximum and overlaid at their IF power null voltage. It can be seen that smaller zero-bias capacitances result in deeper IF power nulls.

be shown experimentally. As can be seen from Fig. 9, the depth of the measured IF power nulls depends strongly on the size of the zero-bias capacitance. For comparison, the IF power for each curve has been normalized to its individual maximum and has been plotted so that the IF power null voltages overlap. It can be seen that a smaller zero-bias capacitance results in a deeper minimum in the IF power. For the diode with the smallest zero-bias capacitance (0.15 fF), an overall depth of the IF power null of as much as 36 dB could be measured.

Thus far, the embedding impedance Z_e has been set to 50 Ω for the calculated curves at all SB frequencies. This is certainly not the case for real diodes under normal measurement conditions. On the other hand, as has been shown in the previous sections, complex (conductive or capacitive) values in the conversion formalism do alter the shape of the IF power curves. This is especially true for the depth of the IF power null. Thus, in order to compare measured curves with calculated curves, the correct embedding impedances have to be considered. Obviously, it is not possible to measure directly diode embedding impedances at terahertz frequencies. Therefore, another approach has been undertaken. Due to the fact that the embedding impedances are the only parameters in the model that cannot be measured directly or deduced from measured values, they have been taken

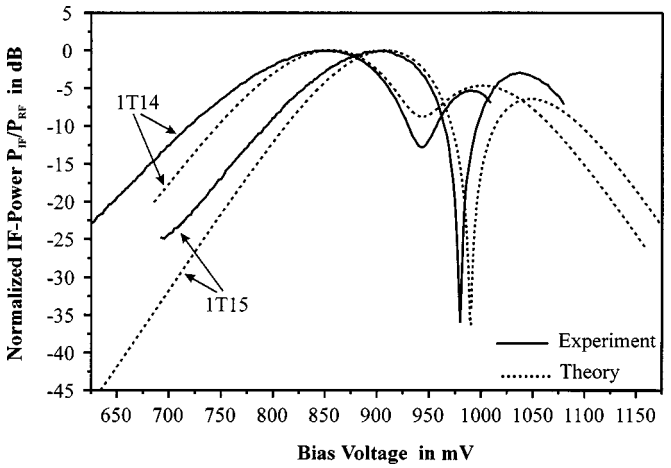

Fig. 10. Measured (solid line) and calculated (dotted line) normalized IF power as a function of bias voltage for diodes of types 1T14 and 1T15.

as modeling parameters. Calculated curves have been produced for various imaginary parts of the embedding impedances until a reasonable match between calculated and measured curves has been achieved. In order not to end up with many unknown parameters, the same embedding impedance has been used at all higher harmonic SBs. It has been found that the real part of the embedding impedances do not have a great influence on the depth and voltage position of the IF power null. Therefore, the embedding impedance at the IF was set to 300 Ω, whereas the real part for all other embedding impedances was kept at 50 Ω.

The results of this curve fitting for two different diodes, i.e., 1T14 with a large zero-bias capacitance and diode 1T15 with a small zero-bias capacitance, can be seen in Fig. 10. Similar curves have been obtained for all the diodes in Table I. Keeping in mind the uncertainties and simplifications made, good matching of measured and calculated curves can be observed.

Generally speaking, it must be stated that all expressions in (8), which add an imaginary contribution to the diode's conductance, have an effect on the admittance matrix element and, therefore, on the conversion loss. This has been pointed out for the diode's capacitance and embedding impedances, respectively, but it is also true for the frequencies involved. The IF is small compared to the LO frequency and its impact can, therefore, be neglected. The LO frequency, in contrast, has an effect on the IF null depth. It has been found experimentally that repeating the same mixing experiment with the same diodes, but using an LO frequency of 1267 GHz (and an RF of 2523 GHz) in contrast to 693 GHz, yields shallower conversion nulls. This is consistent with theory of the dependency of the depth of the IF power null on the relationship between real and imaginary contributions to the admittance and is due to the higher LO frequency connected with the imaginary part in (8).

C. Higher Order Harmonic Mixers

Unfortunately, no appropriate far-infrared laser lines were available to measure the IF power null for a third harmonic mixer. Instead, a fourth harmonic mixing experiment has been carried out with a klystron as the LO at a frequency of 171.8 GHz and a far-infrared laser source radiating at 693 GHz acting as the signal source. It can be seen in Fig. 11 that three

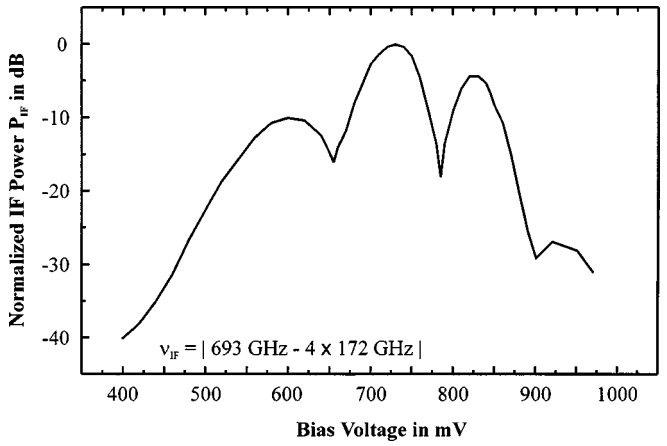

Fig. 11. Measured normalized IF power curve as a function of bias voltage for a fourth harmonic mixer. The phenomenological law that an Nth harmonic mixer reveals $N-1$ IF power minima has been confirmed.

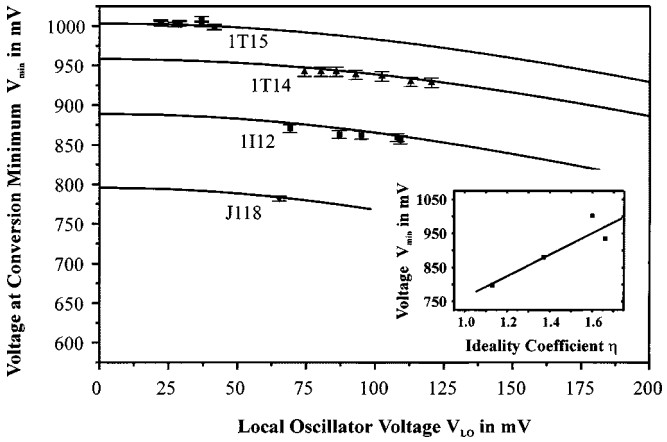

Fig. 12. Measured (solid lines) and calculated (symbols) bias voltages at the IF power null for different diodes versus LO voltage. The inlet shows the strong dependency of the IF power null voltage on the diode's ideality factor.

TABLE II
DIODE PARAMETERS DERIVED FROM *I-V* MEASUREMENTS USED TO COMPARE MEASURED AND CALCULATED IF POWER NULL VOLTAGES IN FIG. 12. THE DIODES' EMBEDDING IMPEDANCES CANNOT BE MEASURED AND ARE, THEREFORE, SET ARBITRARILY TO $Z_e = 50 + i0\ \Omega$

Diode name	Series resistance	Saturation current	Ideality coefficient	Embedding impedance (fixed)
	R_s in Ω	I_s in A	η	Z_e in Ω
1I12	30.0	3.6×10^{-15}	1.37	$50 + i\,0$
J118	27.0	3.5×10^{-16}	1.13	$50 + i\,0$
1T14	14.4	9.0×10^{-14}	1.66	$50 + i\,0$
1T15	24.2	1.1×10^{-14}	1.60	$50 + i\,0$

IF power minima arise for this fourth harmonic mixer. This is further evidence for the above-mentioned $N-1$ law.

D. Voltage Position

The bias voltage at the IF power null $V_{\min}$ has been plotted as a function of the LO power for four different diodes in Fig. 12. $V_{\rm LO}$ has been calculated from the measured bias voltage drop induced by the LO while maintaining a constant bias current in the diode. The relevant diode parameters can be found in Table II. As can be seen from Fig. 12, $V_{\min}$ does slightly depend on the LO power. On the other hand, a much stronger dependency on the diode's ideality coefficient η can be seen, as suggested by (17). It has to be stated that an excellent match of the predicted and measured IF power null voltages is found, though several approximations and simplifications have been made in the theoretical model.

IV. CONCLUSION

The mixing behavior of single Schottky diode harmonic mixers has been investigated analytically and experimentally. It has been shown through laser–laser and laser–klystron mixing experiments that Nth harmonic mixers produce $N-1$ minima of the IF power when the diode bias voltage is varied. This has been confirmed by a simplified analytical description for a second and third harmonic mixer and through experimental results with a second and fourth harmonic mixer. The reason for these conversion loss minima is a cancellation of power due to the competition of different mixing paths. The depth of the IF power null depends strongly on the diode barrier capacitance, imaginary part of the embedding impedance, and related mixing frequencies. This latter effect can be explained by the fact that by introducing nonimpedance components causes the complex impedance matrix element not to go through zero anymore at the IF null bias voltage and, thus, leads to a reduced conversion resonance. Furthermore, approximate formulas have been presented for predicting the bias voltage where the IF power minimum occurs for a second harmonic mixer. Comparison of measured and calculated curves shows good agreement.

REFERENCES

[1] H.-P. Röser, "Heterodyne spectroscopy for submillimeter and far-infrared wavelengths from 100 μm to 500 μm," *Infrared Phys.*, vol. 32, pp. 385–497, 1991.

[2] H.-P. Röser, R. U. Titz, G. W. Schwaab, and M. F. Kimmitt, "Current-frequency characteristics of submicron GaAs Schottky barrier diodes with femtofarad capacitance," *J. Appl. Phys.*, vol. 72, no. 7, pp. 3194–3197, 1992.

[3] H.-P. Röser, H.-W. Hübers, E. Bründermann, and M. F. Kimmitt, "Observation of mesoscopic effects in Schottky diodes at 300 K when used as mixers at THz frequencies," *Semiconduct. Sci. Technol.*, vol. 11, pp. 1328–1332, 1996.

[4] R. U. Titz, H.-P. Röser, G. W. Schwaab, T. W. Crowe, and W. B. Peatman, "Performance of GaAs Schottky barrier diodes as mixers in the THz range," in *SPIE Conf. Dig.*, vol. 1514, R. J. Temkin, Ed., Orlando, FL, 1990.

[5] R. Titz, "Untersuchung von GaAs-Schottky-dioden mit submillimeter-lasern," Faculty Math. Natural Sci., Ph.D. dissertation, Univ. Bonn, Bonn, Germany, 1991.

[6] D. W. Porterfield, "Subharmonically pumped mixers at submillimeter wavelengths," Dept. Elect. Eng., M.S. thesis, Univ. Virginia, Charlottesville, VA, 1994.

[7] R. Feinäugle, *Untersuchungen zum Mischverhalten von Submikron GaAs Schottky-Dioden im THz-Frequenzbereich*. Berlin, Germany: Mensch & Buch Verlag, 1999.

[8] E. Sakuma and K. M. Evenson, "Characteristics of tungsten-nickel point contact diodes used as laser harmonic-generator mixers," *IEEE J. Quantum Electron.*, vol. QE-10, pp. 599–603, Aug. 1974.

[9] J. L. Hesler, D. Kurtz, and R. Feinäugle, "The cause of conversion efficiency nulls for single-diode harmonic mixers," *IEEE Microwave Guided Wave Lett.*, vol. 10, pp. 532–534, Dec. 1999.

[10] D. N. Held and A. R. Kerr, "Conversion loss and noise of microwave and millimeter-wave mixers: Part I—Theory," *IEEE Trans. Microwave Theory Tech.*, vol. MTT-26, pp. 49–55, Feb. 1978.
[11] P. H. Siegel and A. R. Kerr, "Computer analysis of microwave and millimeter-wave mixer," *IEEE Trans. Microwave Theory Tech.*, vol. MTT-28, pp. 275–276, Mar. 1980.
[12] H. C. Torrey and C. A. Whitmer, *Crystal Rectifiers*, ser. MIT Rad. Lab. 15. New York: McGraw-Hill, 1948.
[13] E. H. Rhoderick and R. H. Williams, *Metal–Semiconductor Contacts*, 2nd ed. Oxford, U.K.: Clarendon, 1988.
[14] W. C. B. Peatman and T. W. Crowe, "Design and fabrication of 0.5 micron GaAs Schottky barrier diodes for low-noise terahertz receiver applications," *Int. J. Infrared Millim. Waves*, vol. 11, no. 3, pp. 355–365, 1990.
[15] T. W. Crowe, R. J. Mattauch, H. P. Röser, W. L. Bishop, W. C. B. Peatman, and X. Liu, "GaAs Schottky diodes for THz mixing applications," *Proc. IEEE*, vol. 80, pp. 1827–1841, Nov. 1992.

Roland Feinäugle was born in Überlingen, Germany, on June 3, 1966. He received the Diploma and Ph.D. degrees from the Technical University of Berlin, Berlin, Germany, in 1995 and 1999, respectively, both in physics.

From 1994 to 1995, he was involved with ultrashort pulse laser spectroscopy at the Optics Institute, Technical University of Berlin. From October 1995 to February 1999, he was with the Institute of Space Sensor Technology, German Aerospace Center (DLR), Berlin, Germany, where his main interest was the investigation of Schottky barrier diodes for terahertz heterodyne receivers, as well as laser technology. In 1997, he was a Visiting Research Assistant at the University of Virginia, Charlottesville. Since March 1999, he has been involved with technical astronaut training at the European Astronaut Centre, Cologne, Germany.

Heinz-Wilhelm Hübers received the Diploma degree in physics and the Ph.D. degree from the University of Bonn, Bonn, Germany, in 1991 and 1994, respectively.

From 1991 to 1994, he was with the Max-Planck Institute for Radioastronomy, Bonn, Germany. He then joined the Institute for Space Sensor Technology and Planetary Exploration, German Aerospace Center (DLR), Berlin, Germany, where he is currently the Head of the Heterodyne and Lasertechnolgy Group. His research interests are terahertz heterodyne receivers and their associated technology and physics. He is particularly interested in the development of mixers and lasers for the terahertz frequency range, which includes Schottky diode mixers, superconducting hot electron bolometric mixers, and solid-state lasers based on p-Ge and Si. He is currently involved in the development of a heterodyne receiver for 4.7 THz as part of the German heterodyne receiver for the Stratospheric Observatory for Infrared Astronomy (SOFIA).

Hans Peter Röser was born in Polch, Germany, on October 8, 1949. He received the Diploma degree in physics and the Ph.D. degree from the University of Bonn, Bonn, Germany, in 1976 and 1979, respectively.

He was with the Max-Planck-Institute for Radioastronomy, where he held a number of positions in the Department of Millimeter and Submillimeter/Far-Infrared Technology. He has carried out studies and development work on high-resolution low-noise heterodyne spectrometers, which were used in ground-based telescopes and on board the National Aeronautics and Space Administration's (NASA) Kuiper Airborne Observatory. Since 1994, he has been the Director of the Institute of Space Sensor Technology, German Aerospace Center (DLR), Berlin, Germany, and a Professor at the Technical University of Berlin, Berlin, Germany. He has authored or co-authored over 50 papers in international journals. His main interest is the development and application of remote sensing instruments in the visible and infrared wavelength range for airborne and space-borne programs.

Dr. Röser has received several awards in physics and engineering.

Jeffrey L. Hesler (S'88–M'89) was born in Seattle, WA, on July 8, 1966. He received the B.S.E.E. from the Virginia Polytechnic Institute, Blacksburg, in 1989, and the M.S.E.E. and Ph.D. degrees from the University of Virginia, Charlottesville, in 1991 and 1996, respectively.

Since 1996, he has been with the Department of Electrical Engineering, University of Virginia, initially as a Research Scientist, and since 1997, as a Research Assistant Professor. His research interests include millimeter- and submillimeter-wave device and circuit design, modeling, and testing. His current research projects include the development of compact room-temperature harmonic mixers at submillimeter wavelengths and the use of various micromachining and molding techniques in the fabrication of submillimeter-wavelength components.